FAM29A promotes microtubule amplification via recruitment of the NEDD1–γ-tubulin complex to the mitotic spindle

Hui Zhu,[1] Judith A. Coppinger,[3] Chang-Young Jang,[1] John R. Yates III,[3] and Guowei Fang[1,2]

[1]Department of Biological Sciences, Stanford University, Stanford, CA 94305
[2]Genentech, Inc., South San Francisco, CA 94080
[3]Department of Chemical Physiology, The Scripps Research Institute, La Jolla, CA 92037

Microtubules (MTs) are nucleated from centrosomes and chromatin. In addition, MTs can be generated from preexiting MTs in a γ-tubulin–dependent manner in yeast, plant, and *Drosophila* cells, although the underlying mechanism remains unknown. Here we show the spindle-associated protein FAM29A promotes MT-dependent MT amplification and is required for efficient chromosome congression and segregation in mammalian cells. Depletion of FAM29A reduces spindle MT density. FAM29A is not involved in the nucleation of MTs from centrosomes and chromatin, but is required for a subsequent increase in MT mass in cells released from nocodazole. FAM29A interacts with the NEDD1–γ-tubulin complex and recruits this complex to the spindle, which, in turn, promotes MT polymerization. FAM29A preferentially associates with kinetochore MTs and knockdown of FAM29A reduces the number of MTs in a kinetochore fiber, activates the spindle checkpoint, and delays the mitotic progression. Our study provides a biochemical mechanism for MT-dependent MT amplification and for the maturation of kinetochore fibers in mammalian cells.

Introduction

The mitotic spindle, a dynamic assembly of microtubules (MTs) polymerized from the α/β-tubulin subunit, controls accurate chromosome segregation during cell division (Wittmann et al., 2001; Scholey et al., 2003). MT-associated proteins, such as motor and nonmotor proteins, act together to orchestrate the assembly, dynamics, and function of the spindle and the congression and segregation of chromosomes in mitosis (Karsenti and Vernos, 2001; Gadde and Heald, 2004; Kline-Smith and Walczak, 2004). Among these proteins, factors that nucleate MTs are most important ones, as they initiate spindle assembly and maintain MT density (Wiese and Zheng, 2006).

At least two well-characterized pathways control MT nucleation and spindle assembly in mitosis (Gadde and Heald, 2004). In one pathway, centrosomes recruit factors to nucleate astral as well as spindle MTs. The plus end of individual spindle MT grows and shrinks to "search and capture" individual chromosomes, leading to the attachment of a single MT to a kinetochore (Kirschner and Mitchison, 1986; Maiato et al., 2004). How a single attached MT is quickly matured into a kinetochore fiber of 25–30 MTs (McIntosh et al., 2002) remains as one of the most important questions unanswered in cell biology. The second pathway is mediated through a chromatin-dependent nucleation activity (Wilde and Zheng, 1999; Gadde and Heald, 2004). The chromatin-associated guanine nucleotide exchange factor, RCC1, promotes the formation of a gradient of Ran-GTP in the vicinity of mitotic chromatin (Bastiaens et al., 2006), which, in turn, activates spindle assembly factors to promote nucleation (Karsenti and Vernos, 2001) and stabilization (Gruss and Vernos, 2004; Jang et al., 2008) of MTs around chromosomes. Other mechanisms also contribute to the formation of MTs (O'Connell and Khodjakov, 2007). For example, it has been demonstrated that MTs can grow from the side of existing MTs in plant cells (Murata et al., 2005) and in yeast (Janson et al., 2005) to amplify cytoskeleton structure locally in interphase, although the molecular mechanism for this phenomenon remains unknown. Very recently, the *Drosophila* Augmin complex has been shown to be

Correspondence to Guowei Fang: fang.guowei@gene.com

Abbreviations used in this paper: FLIP, fluorescence loss in photobleaching; MT, microtubule; Plk1, polo-like kinase 1.

The online version of this article contains supplemental material.

The Rockefeller University Press $30.00
J. Cell Biol. Vol. 183 No. 5 835–848
www.jcb.org/cgi/doi/10.1083/jcb.200807046

required for centrosome-independent MT generation within the spindle in culture cells (Goshima et al., 2008).

Nucleation of MTs from centrosomes is mediated by a MT nucleator, the γ-tubulin ring complex (γTuRC) (Wiese and Zheng, 2006). γTuRC is recruited to centrosomes, where γ-tubulin promotes the polymerization of α/β-tubulin subunits into MT polymers. During mitosis, γTuRC is localized to both centrosomes and to spindle MTs and a regulatory protein, NEDD1, interacts with γ-tubulin and targets γTuRC to these mitotic structures (Haren et al., 2006; Luders et al., 2006). In addition, NEDD1 and γTuRC are required for chromatin-mediated nucleation of MTs and the NEDD1–γTuRC complex is targeted to multiple foci on chromatin to promote MT polymerization in mitotic cells released from a nocodazole arrest (Luders et al., 2006). The mechanism for the recruitment of NEDD1 in mitosis remains unknown (Luders et al., 2006).

The Polo-like kinase 1 (Plk1) is a mitotic kinase that regulates spindle assembly and mitotic progression (Barr et al., 2004; van Vugt et al., 2004; Petronczki et al., 2008). In a proteomic study on the function and regulation of Plk1 (Seki et al., 2008a, b), we identified human FAM29A (family with sequence similarity, member 29A) as a novel Plk1-interacting protein. We report here that FAM29A is a MT-associated protein that preferentially associates with kinetochore MTs (k-MTs). Depletion of FAM29A reduces the spindle MT density, including that of k-MTs, weakens the MT–kinetochore attachment, and activates the spindle checkpoint. We demonstrated that FAM29A interacts with the NEDD1–γ-tubulin complex and is responsible for recruiting this complex to the mitotic spindle where γ-tubulin promotes the polymerization of additional MTs in a manner independent of centrosomes and chromatin. The FAM29A–NEDD1 pathway controls the MT-dependent MT polymerization, a process important for the assembly of the spindle, for the maturation of k-MTs, and for normal progression of mitosis in mammalian cells.

Results

FAM29A is a novel spindle protein preferentially associated with kinetochore MTs

To study the function and regulation of Plk1, we previously purified the Plk1 complexes from mitotic HeLa S3 cells and identified its associated proteins by mass spectrometry (Seki et al., 2008a, b). One of the Plk1-binding proteins discovered was FAM29A (14 peptides identified from 3 independent purifications [unpublished data]), a protein that shares a weak sequence homologue to the Dgt6 subunit of the *Drosophila* Augmin complex (32% aa identity over a 100-aa region) (Goshima et al., 2008). We raised and affinity purified an anti-FAM29A antibody, which recognized both the endogenous and ectopically expressed FAM29A (Fig. S1 A, available at http://www.jcb.org/cgi/content/full/jcb.200807046/DC1). In a coimmunoprecipitation experiment, we confirmed that endogenous Plk1 interacted with FAM29A (unpublished data). The functional importance of this interaction will be reported in a future study.

We analyzed the expression of FAM29A in the cell cycle. HeLa S3 cells were arrested at the G1/S boundary by a double-thymidine treatment, and then released into fresh media (Fang et al., 1998a, b). The cell cycle profile was determined by fluorescence-activated cell sorting (FACS) and protein levels were analyzed by Western blotting. The FAM29A protein was present in G1, S, and G2, and its levels were increased in M. Mitotic FAM29A migrated slower at a time point right before degradation of cyclin B (Fig. 1 A; also see Fig. 5 D). This form of FAM29A is hyperphosphorylated, as its mobility was restored by a treatment with λ-phosphatase (see Fig. 5 B; unpublished data).

We analyzed the cellular localization of FAM29A (Fig. 1 B). At early prometaphase, FAM29A colocalized with MTs within the boundary defined by condensed chromosomes, whereas MTs polymerized in all directions around DNA. From late prometaphase to metaphase FAM29A associated with the mitotic spindle, and from anaphase to cytokinesis it also colocalized with central spindle and midbody MTs (Fig. 1 B). In interphase, FAM29A was presented at centrosomes where it colocalized with or was adjacent to centrin at centrioles. This centrosomal localization is independent of MTs. Depolymerization of MTs by nocodazole in mitotic cells revealed that FAM29A is preferentially associated with one of the centrioles in the mitotic centrosome (Fig. 1 B). The specificity of FAM29A localization was confirmed by expression of GFP-FAM29A and by depletion of FAM29A (Fig. 1 C; also see Fig. 3 A; unpublished data).

FAM29A associated with k-MTs (Fig. 1, D–F; Fig. S1, B and C). When the monopolar spindle was formed by monastrol, an Eg5 inhibitor (Mayer et al., 1999), FAM29A localized on MTs within the chromosome sphere, but not on the long MTs that extended beyond chromosomes (Fig. 1 D). Co-staining of FAM29A with Hecl revealed that FAM29A-positive MTs almost invariably ended at, but did not extend beyond, the Hecl-positive kinetochores (Fig. 1 E). Incubation of HeLa cells at 4°C removed unstable MTs in the spindle, resulting in a decrease in MT density (Fig. 1 F). The remaining MTs after a 10-min incubation at 4°C are cold-resistant k-MTs. Interestingly, FAM29A intensity in the spindle remained stable during the incubation, whereas the spindle MT intensity decreased dramatically from 0 min to 10 min after shifting from 37°C to 4°C (Fig. 1 F). Furthermore, FAM29A remained colocalized with spindle MTs in metaphase cells incubated at 4°C for 10 min (unpublished data). Thus, FAM29A preferentially associated with cold-resistant k-MTs. Consistent with this, depletion of the kinetochore protein Nuf2 greatly reduced the spindle-associated FAM29A signals (Fig. S1, B and C), as depletion of Nuf2 prevents stable MT–kinetochore interaction (DeLuca et al., 2002). Mitotic phosphorylation of FAM29A and its colocalization with k-MTs suggested that FAM29A is a novel MT-associated protein acting in mitosis.

FAM29A is required for mitotic progression

To investigate the function of FAM29A in mitosis, we analyzed the kinetics of mitotic progression in HeLa cells depleted of FAM29A. Two independent siRNAs each reduced the FAM29A protein by 90% (Fig. 2 A, top) and gave a similar phenotype. Depletion of FAM29A by siRNAs increased the mitotic index by two- to fourfold (Fig. S2, A and B; available at

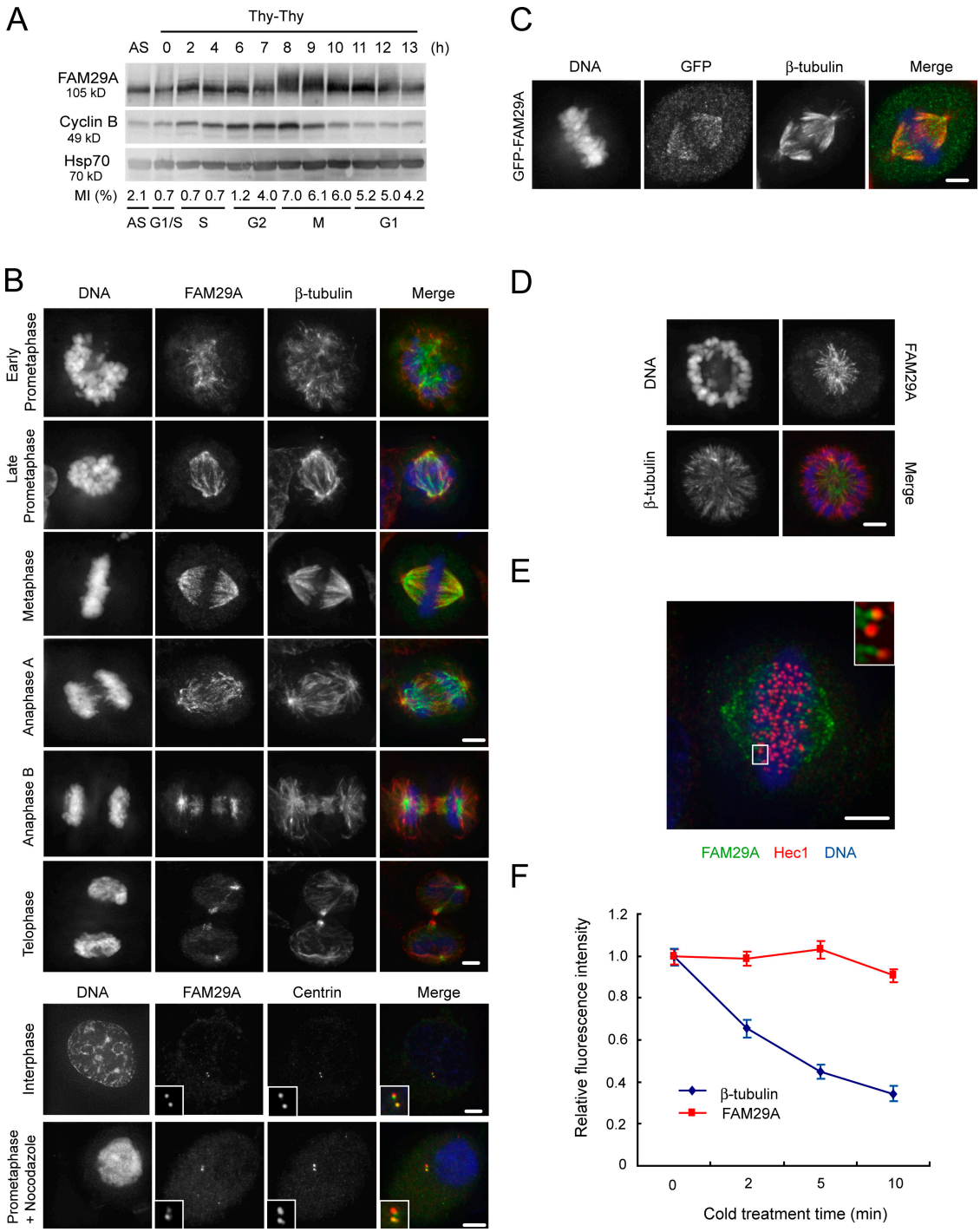

Figure 1. **FAM29A is a spindle protein preferentially associated with kinetochore MTs.** (A) HeLa S3 cells were synchronized at the G1/S boundary by a double-thymidine arrest and harvested at the indicated time after release. Cell cycle profile was analyzed by FACS with anti-MPM2 antibody staining and propidium iodide staining. Protein levels were determined by Western blotting with Hsp70 as a loading control. (B–E) Maximum projections from deconvolved z stacks of representative HeLa cells (B, D, and E) or a HeLa cells transiently expressing GFP-FAM29A (C). Cells were stained for FAM29A (B, D, and E)/GFP (C) (green), β-tubulin (B–D)/centrin (B)/Hec1 (E) (red), and DNA (blue). In D, the cell was incubated with Monastrol (4 µM) for 4 h and then stained. The inset in E shows a single focal plane of the boxed region. (F) HeLa cells were cultured at 37°C and then incubated at 4°C for the indicated time. Cells were stained for FAM29A, β-tubulin, and DNA. MT and FAM29A fluorescence intensity in the mitotic spindle of metaphase cells (n = 10 cells for each time point) were quantified and normalized to their respective intensity at the 0-min time point. Error bars, SEM. Bars, 5 µm.

http://www.jcb.org/cgi/content/full/jcb.200807046/DC1). This phenotype is specific, as transfection of an siRNA targeting to the 3′ untranslated region of FAM29A (siFAM29A-B) into a cell line stably expressing GFP-FAM29A (HeLa/GFP-FAM29A) did not affect the expression of transgene and rescued the mitotic phenotype (Fig. 2 A; Fig. S2, A and B).

Among mitotic cells, depletion of FAM29A led to an increase in metaphase cells (Fig. S2 B), indicating that FAM29A

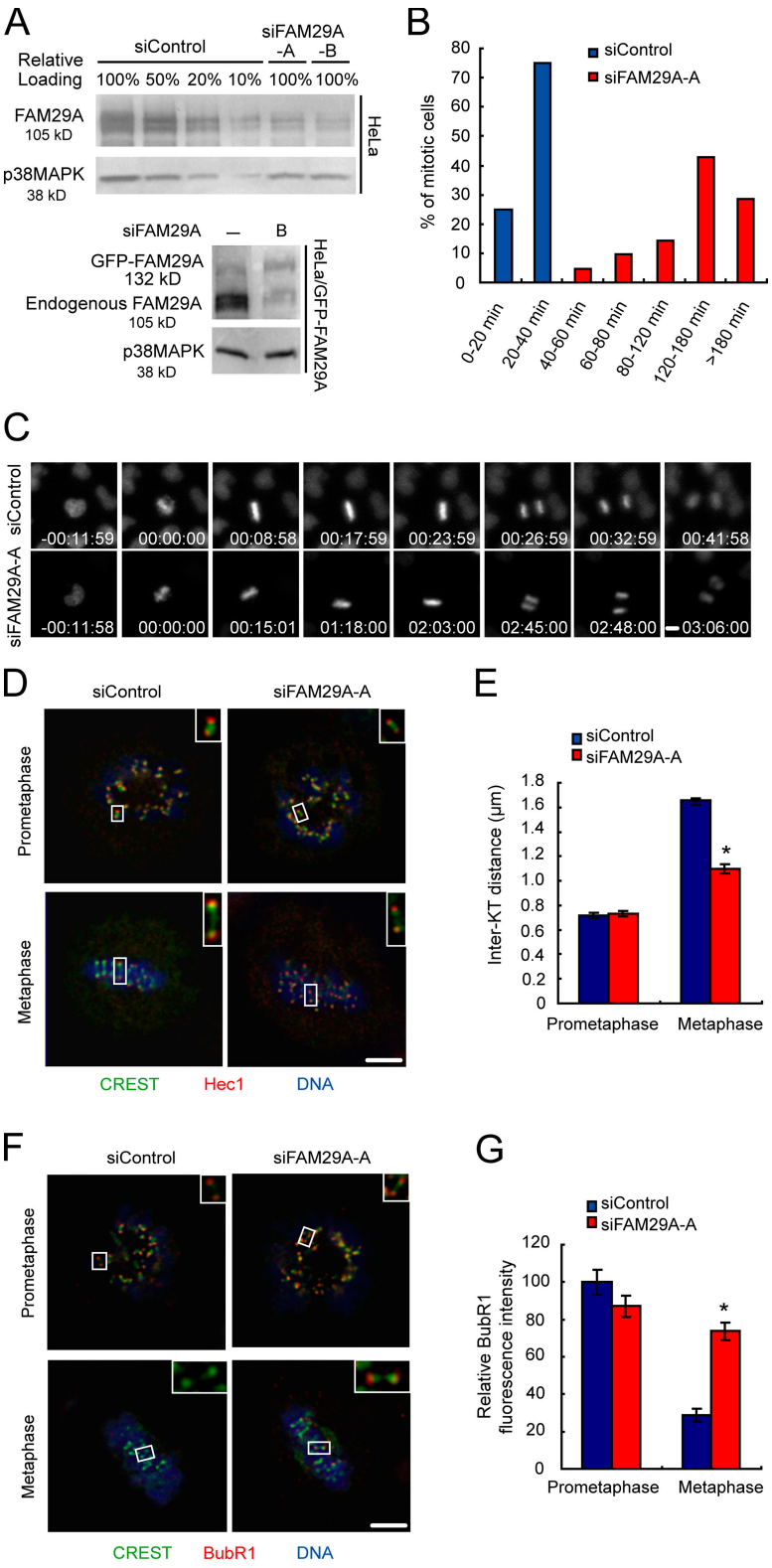

Figure 2. **FAM29A controls mitotic progression.** (A) HeLa cells and HeLa/GFP-FAM29A cells were transfected with either control (siControl) or FAM29A-specific siRNAs (siFAM29A-A and B) and analyzed by Western blotting. (B and C) HeLa/GFP-H2B cells were transfected with siRNAs and imaged for GFP by time lapse, starting from 50 h after transfection. Cell images were captured every 3 min to monitor mitotic progression. Representative still images are shown in C and the time stamp is in h:min:s (Video 1 for siControl, and Video 2 for siFAM29A-A; Videos available at http://www.jcb.org/cgi/content/full/jcb.200807046/DC1). The time when a cell enters metaphase is set to 0 min. Mitotic cells were divided into different categories based on the duration of metaphase (from the initial metaphase plate formation to anaphase onset) (30 cells quantified for each transfection) (B). (D–G) A single focal plane from deconvolved z stacks of representative HeLa cells transfected with siRNAs and stained for CREST (green), Hec1 (D)/BubR1 (F) (red), and DNA (blue). Insets show the details of the boxed regions. Inter-kinetochore (Inter-KT) distances (E; $n > 100$ kinetochore pairs from five cells for each quantification) and kinetochore BubR1 signals (G; $n = 100$ kinetochores) in prometaphase and metaphase cells were quantified and plotted. In E: *, $P < 4.7 \times 10^{-24}$; in G: *, $P < 5.0 \times 10^{-4}$ (two-tailed *t* test relative to siControl metaphase cells). Error bars, SEM. Bars: 10 μm (C); 5 μm (D and F).

controls mitotic progression. We analyzed the kinetics of mitotic progression by time-lapse imaging of HeLa cells stably expressing GFP-histone H2B (HeLa/GFP-H2B). Depletion of FAM29A greatly increased the duration of metaphase (Fig. 2, B and C). Although control metaphase cells all initiated anaphase within 40 min after chromosome alignment (Video 1, available at http://www.jcb.org/cgi/content/full/jcb.200807046/DC1), not a single metaphase cell depleted of FAM29A segregated its chromosomes within this time frame and the majority of depleted cells stayed at metaphase for over 120 min (Video 2) (Fig. 2 B).

This prolonged metaphase in siFAM29A cells resulted from a less efficient capture of chromosomes and a lack of tension on

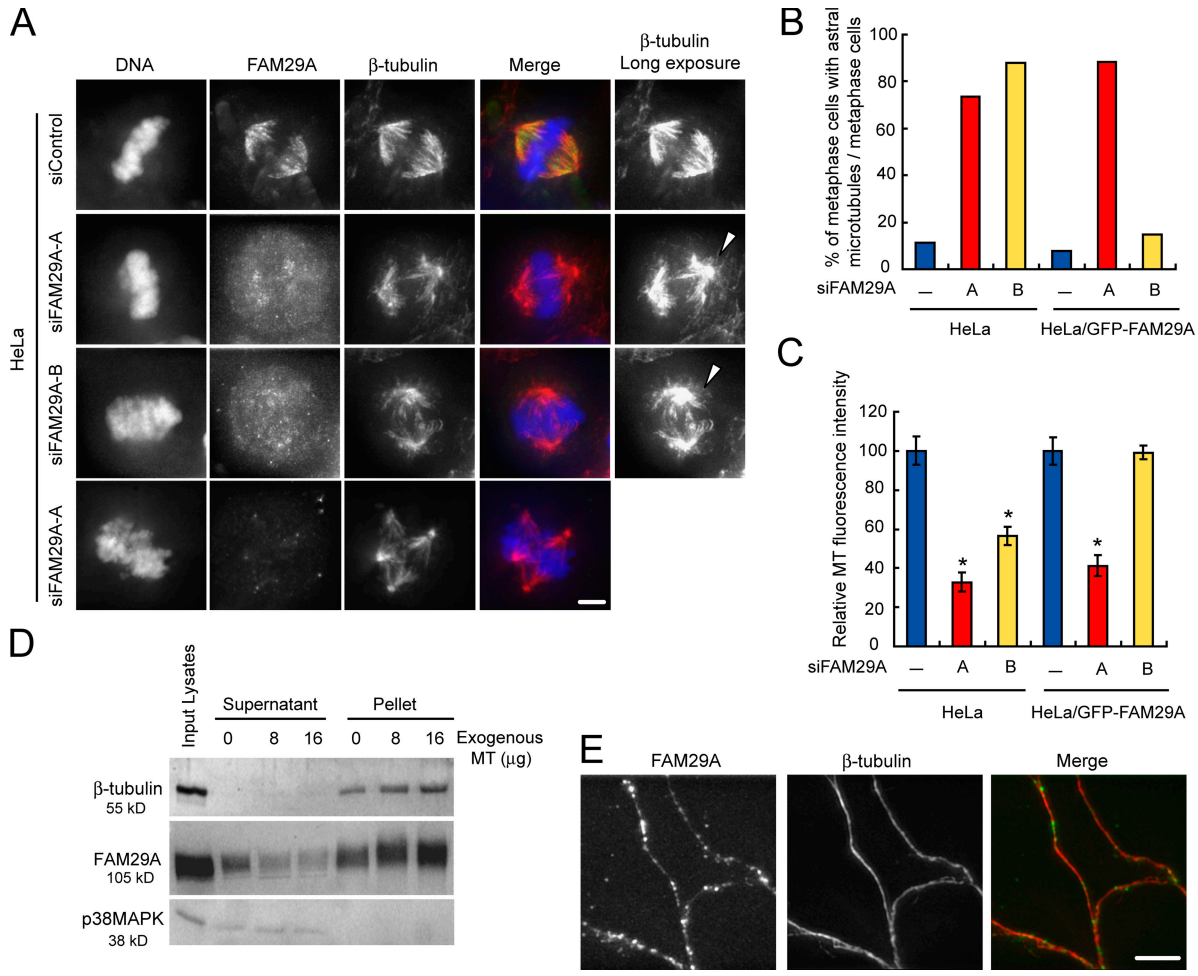

Figure 3. **FAM29A controls spindle structure.** (A–C) Maximum projections from deconvolved z stacks of representative HeLa cells transfected with siRNAs and stained for FAM29A (green), β-tubulin (red), and DNA (blue). Long exposures of the β-tubulin images are presented here to show the increased amounts of astral MTs. Arrowheads point to astral MTs outside spindle poles. The percentage of metaphase cells with detectable astral MTs among total metaphase cells (B; *n* = 100 cells for each quantification) as well as the MT fluorescence intensity in metaphase cells (C; *n* = 10 cells) were quantified and plotted. In C: *, P < 0.01 (two-tailed *t* test relative to siControl metaphase cells). (D) Lysates of prometaphase HeLa S3 cells were incubated with increasing amounts of exogenously added, taxol-stabilized MTs, followed by sedimentation of MTs. Pellets and supernatants were analyzed by Western blotting. (E) Lysates of prometaphase HeLa S3 cells were incubated with taxol-stabilized MTs, fixed, centrifugated onto coverslips, and stained for FAM29A (green) and β-tubulin (red). Error bars, SEM. Bars, 5 μm.

kinetochores of aligned chromosomes. Among metaphase cells, over 25% siFAM29A cells had chromosomes unaligned outside the metaphase plate, compared with <1% in control cells (Fig. S2 C). Even for chromosomes aligned at the metaphase plate, the pulling force, or tension, generated by attached MTs across sister kinetochores was substantially reduced in siFAM29A cells, as indicated by a shorter inter-kinetochore distance in metaphase cells (Fig. 2, D and E). Confocal time-lapse microscopy in HeLa cells stably expressing GFP-CenpA (HeLa/GFP-CenpA) (Fig. S2 D; Videos 3 and 4, available at http://www.jcb.org/cgi/content/full/jcb.200807046/DC1) indicated that depletion of FAM29A not only reduced the inter-kinetochore distance, but also attenuated the movement of sister kinetochores relative to each other, another indicator for the lack of pulling force from attached MTs. Consistent with a lack of tension, the kinetochore-associated BubR1 signals were twofold higher on aligned chromosomes in FAM29A-depleted metaphase cells than those in control cells (Fig. 2, F and G), indicating that the spindle checkpoint (Pinsky and Biggins, 2005; Musacchio and Salmon, 2007) is active in metaphase cells depleted of FAM29A.

FAM29A controls spindle structure and function

Given the association of FAM29A with the spindle and its function in mitosis, we investigated the role of FAM29A in spindle assembly, dynamics, and function. FAM29A controls the MT density within the spindle (Fig. 3, A and C). In FAM29A-depleted cells, the fluorescence intensity of MTs was reduced by ∼50–60% relative to that in control cells (Fig. 3 C).

Depletion of FAM29A also led to a disorganized mitotic spindle with abnormal shape and an increase in the amounts of astral MTs (Fig. 3, A and B; Fig. S3 A, available at http://www.jcb.org/cgi/content/full/jcb.200807046/DC1). Although previous electron microscopic studies indicate that the majority of normal metaphase cells have multiple astral MTs, these astral MTs were usually not detectable under our immunofluorescence

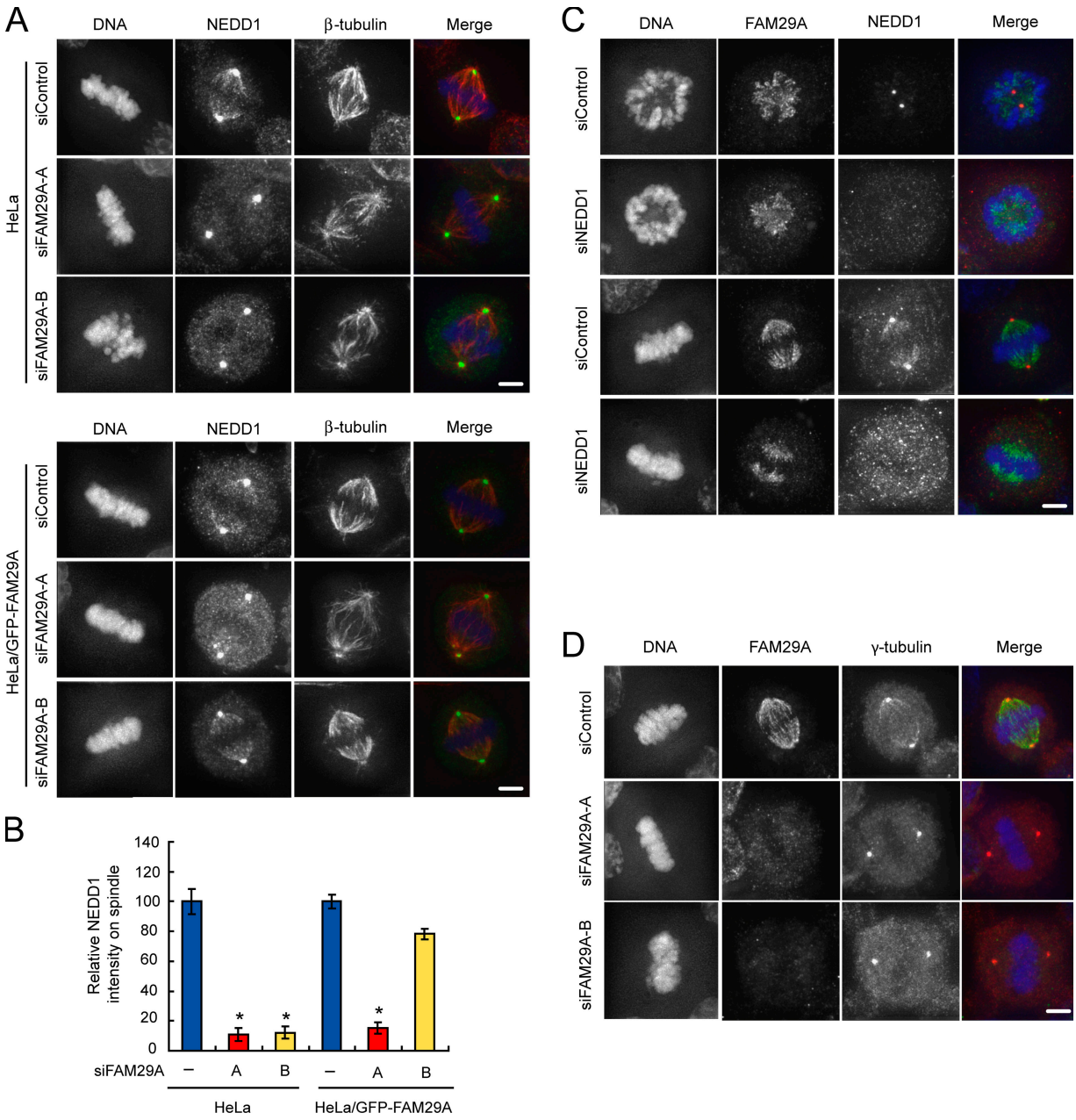

Figure 4. **FAM29A recruits NEDD1 onto spindle MTs.** (A and B) Maximum projections from deconvolved z stacks of representative HeLa or HeLa/GFP-FAM29A cells transfected with siRNAs and stained for NEDD1 (green), β-tubulin (red), and DNA (blue) (A). NEDD1 fluorescence intensity on spindle (excluding spindle pole signals) was quantified (B; $n = 10$ metaphase cells). *, $P < 0.01$ (two-tailed t test relative to siControl metaphase cells). (C and D) Maximum projections from deconvolved z stacks of representative HeLa cells transfected with siRNAs and stained for FAM29A (green), NEDD1 (C)/γ-tubulin (D) (red), and DNA (blue). Error bars, SEM. Bars, 5 μm.

studies due to the fixation and assay conditions (Fig. 3 A). Thus, in control metaphase cells, only 10% metaphase cells have detectable astral MTs under our assay conditions. However, in FAM29A-depleted metaphase cells, the percentage increased to 70–80% (Fig. 3 B). In addition, there is a greater than fivefold increase in FAM29A-depleted mitotic cells with multi-polar spindles compared with control mitotic cells (Fig. S3 B). Interestingly, the majority of FAM29A-depleted cells with multi-polar spindles still had their chromosomes aligned on a metaphase plate (Fig. 3 A), suggesting a possibility that multiple poles in depleted cells resulted from splitting of the spindle poles that occurred after the formation of a bipolar spindle and the alignment of chromosomes. All the phenotypes in siFAM29A cells are specific, as they were rescued in HeLa/GFP-FAM29A cells transfected with siFAM29A-B (Fig. 3, B and C; Fig. S3).

FAM29A is a MT-binding protein (Fig. 3, D and E). In an in vitro MT cosedimentation assay, FAM29A from lysates of mitotic HeLa cells co-pelleted with MTs in a dose-dependent manner (Fig. 3 D). Immunofluorescence staining of pelleted MTs also showed an association of FAM29A with in vitro polymerized MTs along the length of MTs (Fig. 3 E), suggesting that FAM29A binds to the side of MTs.

FAM29A recruits NEDD1 to spindle MTs

A reduction of the spindle MT density in FAM29A-depleted cells suggests a role of FAM29A in promoting MT growth and/or in preventing MT catastrophe. Thus, we analyzed the localization of a number of factors involved in the nucleation or depolymerization of MTs in siFAM29A cells. Although the localization pattern of NuMA, chTOG, TPX2, Kif18A, and MCAK were not affected by depletion of FAM29A (unpublished data), recruitment of NEDD1 to spindle MTs is under the control of FAM29A (Fig. 4 A).

We first determined the localization of NEDD1 and FAM29A in the cell cycle (Fig. S4 A, available at http://www.jcb.org/cgi/content/full/jcb.200807046/DC1). Both were concentrated on centrosomes in interphase cells. During early prometaphase at a time when NEDD1 is still mostly on centrosomes (Haren et al., 2006; Luders et al., 2006), FAM29A becomes associated with newly polymerized MTs. At metaphase, FAM29A and NEDD1 colocalized on the entire mitotic spindle. At anaphase and during cytokinesis, NEDD1 signals on the spindle decreased slightly, whereas FAM29A still associated with the spindle MTs.

Depletion of FAM29A did not alter the level of the NEDD1 protein (Fig. S4 B). However, depletion of FAM29A almost quantitatively removed NEDD1 from spindle MTs without affecting its localization to centrosomes (Fig. 4, A and B). The lack of NEDD1 on spindle MTs is not simply due to a reduction of MTs, as the decrease in the spindle NEDD1 intensity is much more severe than the reduction of spindle MTs in siFAM29A cells (compare Fig. 3 C with Fig. 4 B). We conclude that FAM29A is specifically required for the association of NEDD1 with spindle MTs, but not for its localization to centrosomes.

Next, we analyzed the dependence of FAM29A localization on NEDD1. Efficient depletion of NEDD1 using a previously characterized siRNA arrested cells at early prometaphase (Fig. S4 C and Fig. 4 C), consistent with published reports (Haren et al., 2006; Luders et al., 2006). Cells with partial knockdown of NEDD1 progressed to metaphase with a bipolar spindle. Under both conditions, the localization and the intensity of FAM29A on the mitotic spindle were not affected (Fig. 4 C). Thus, FAM29A acts upstream of NEDD1 to promote its recruitment to the mitotic spindle.

It has been reported that NEDD1 directly interacts with and recruits the γ-tubulin ring complex to centrosomes and to spindle MTs to promote MT nucleation and spindle assembly (Luders et al., 2006). We found that depletion of FAM29A also abolished γ-tubulin signals on the mitotic spindle, but not on centrosomes (Fig. 4 D). Again, depletion of FAM29A did not alter the level of the γ-tubulin protein (Fig. S4 B). We conclude that FAM29A promotes the nucleation of MTs from the spindle through recruitment of NEDD1 and γ-tubulin, and that loss of this nucleation activity leads to a reduction of the MT density and an aberrant mitotic spindle.

FAM29A interacts with NEDD1

To explore whether FAM29A and NEDD1 interact, we investigated the physiological forms of the FAM29A and NEDD1 proteins in mitosis by centrifugation of lysates of mitotic cells through a sucrose-density gradient. Both NEDD1 and γ-tubulin were sedimented into two similar peaks (Luders et al., 2006). Interestingly, FAM29A cosedimented with the low-molecular weight fractions of NEDD1 and γ-tubulin (Fig. S4 D).

Ectopically expressed NEDD1 and FAM29A interact with each other. Myc-tagged NEDD1 was cotransfected with GFP-FAM29A or GFP in HeLa cells. Immunoprecipitation of GFP-FAM29A specifically pulled down myc-NEDD1 (Fig. 5 A). Similarly, endogenous FAM29A also interacted with NEDD1 and γ-tubulin, but only in mitotic cells, not in asynchronous cells, as assayed in a coimmunoprecipitation experiment (Fig. 5 B). Furthermore, only the hyperphosphorylated NEDD1 associated with FAM29A, although mitotic phosphorylation of NEDD1 and FAM29A does not appear to be required for their association, as incubation of the immunoprecipitate with λ-phosphatase did not dissociate the complex (Fig. 5 B).

The association of FAM29A with the NEDD1–γ-tubulin complex is cell cycle regulated. HeLa S3 cells were synchronized at prometaphase by a thymidine-nocodazole treatment and then released for exit from mitosis (Fang et al., 1998a). The FAM29A–NEDD1–γ-tubulin complex peaked in mitosis and was reduced as cells exited into G1 (Fig. 5 C). Alternatively, HeLa S3 cells were synchronized at the G1/S boundary by a double-thymidine treatment and then released (Fang et al., 1998b). Again, the complex between FAM29A and NEDD1–γ-tubulin increased its abundance in G2 and M cells (Fig. 5 D).

FAM29A promotes MT polymerization independent of centrosomes and chromatin

We investigated the role of FAM29A in MT dynamics and spindle assembly. The kinetics of depolymerization of spindle MTs were analyzed by confocal time-lapse microscopy in HeLa cells stably expressing GFP–α-tubulin (HeLa/GFP–α-tubulin). Although spindle MTs in both control and FAM29A-knockdown cells were depolymerized with 1 μg/ml nocodazole within 15 min, the rate of depolymerization was slightly faster in siFAM29A cells (Fig. S5 A; Videos 5 and 6, available at http://www.jcb.org/cgi/content/full/jcb.200807046/DC1). By 120 s after nocodazole treatment, the majority of MTs disappeared in metaphase cells depleted of FAM29A, whereas the bipolar spindle structure was clearly identifiable in control metaphase cells. Direct analysis of the turnover rate of the α/β-tubulin subunit in the metaphase spindle in a fluorescence loss in photobleaching (FLIP) experiment also supports this conclusion (Fig. S5 B). Cytoplasmic GFP–α-tubulin was photobleached continuously while time-lapse imaging recorded the decrease in fluorescence intensity in the metaphase spindle (Videos 7 and 8). In control cells, the half-life of GFP–α-tubulin on the spindle was 122.77 s, whereas the half-life decreased to 101.95 s in FAM29A knockdown cells (Fig. S5 B, insets). Thus, FAM29A has a stabilizing effect to the mitotic spindle.

Next, we examined the role of FAM29A in MT polymerization. Metaphase MTs in control or siFAM29A cells were completely depolymerized with nocodazole and the rate of MT repolymerization was determined by confocal time-lapse microscopy upon release from nocodazole. Within 2–3 min after release, MTs began to regrow from centrosomes in both control and siFAM29A cells (Fig. 6 A; Videos 9 and 10, available at

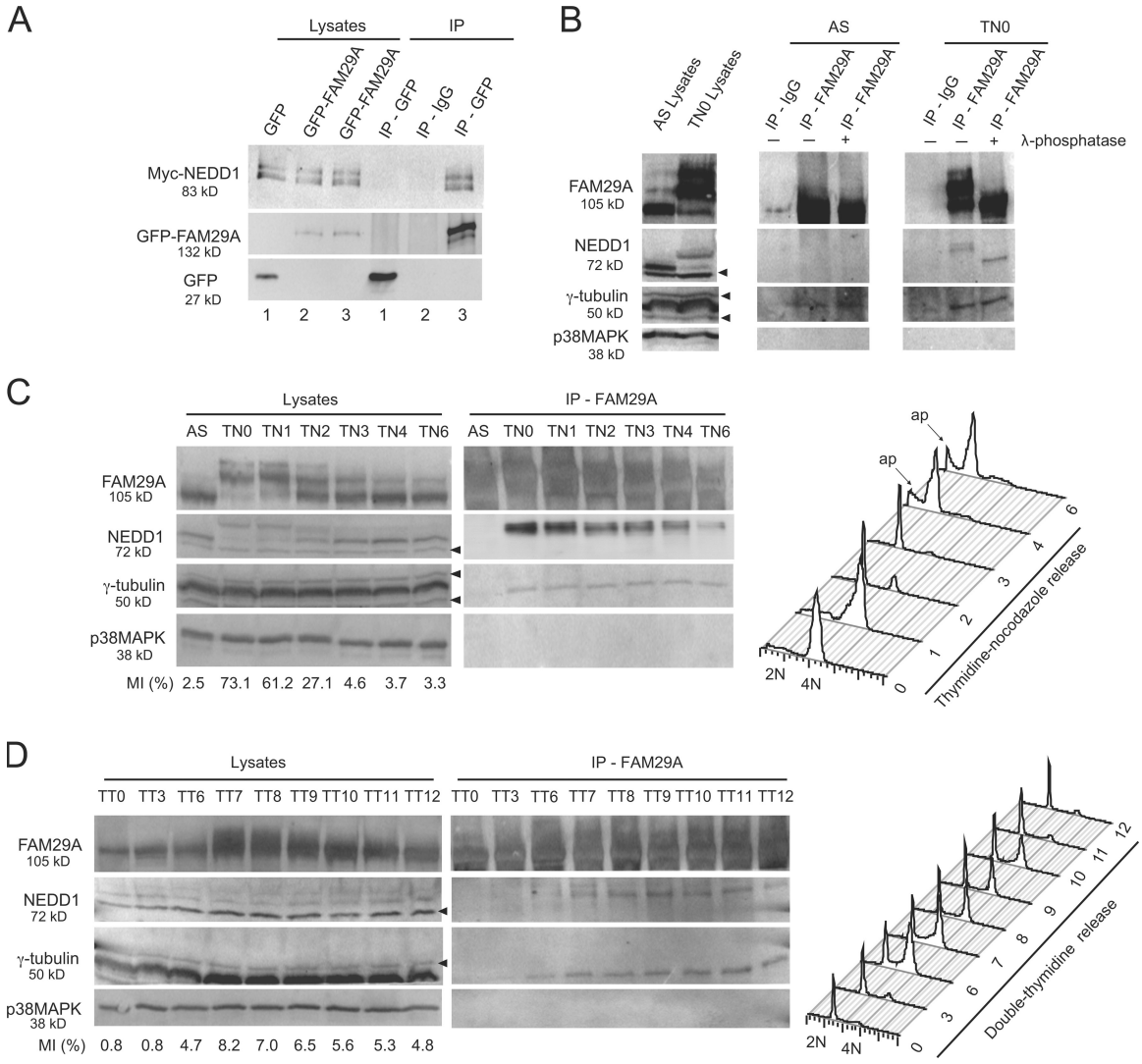

Figure 5. **FAM29A interacts with NEDD1.** (A) Myc-NEDD1 was cotransfected with GFP-FAM29A or GFP into HeLa cells. Lysates of transfected HeLa cells were immunoprecipitated (IP) with anti-GFP antibodies or with nonspecific IgG followed by Western blotting. (B) HeLa S3 cells were synchronized at prometaphase by a thymidine-nocodazole treatment (TN0). Lysates from asynchronous cells (AS) or prometaphase cells were immunoprecipitated with anti-FAM29A antibodies or with nonspecific IgG. The immunoprecipitates were treated with or without λ-phosphatase followed by Western blotting. (C and D) HeLa S3 cells were synchronized at prometaphase by a thymidine-nocodazole treatment (TN) (C) or at the G1/S boundary by a double-thymidine treatment (TT) (D). Cells were released and harvested at the indicated times (hours). Cell cycle profile was determined by FACS. Lysates and the anti-FAM29A immunoprecipitates were analyzed by Western blotting. In B–D, arrowheads point to nonspecific cross-reacting proteins on Western blot. "ap" (in C), apoptotic cells.

http://www.jcb.org/cgi/content/full/jcb.200807046/DC1). At 3–5 min after release, MT foci and fibers also grow from chromatin with similar fluorescence intensity independent of FAM29A depletion. Quantitative analysis of MT immunofluorescence intensity in fixed cells confirmed the results from live cell imaging. The initial rate of MT nucleation and polymerization from centrosomes and chromatin during the first 5 min after release was indistinguishable between control- and FAM29A-depleted cells (Fig. 6, B and C). However, from 7 min on, control cells continued to increase their MT mass almost linearly, whereas cells depleted of FAM29A stopped the growth of MTs and MT mass plateaued by 7 min. In addition, siFAM29A cells formed bipolar spindle much less efficiently (Fig. 6 A; unpublished data). 72% mitotic cells formed bipolar spindles in the control sample by 30 min after release, whereas 30% mitotic cells in the siFAM29A-depleted sample had bipolar spindles at the same time point (n = 80 cells for each quantification).

Our analysis of spindle formation in cells released from nocodazole treatment indicates that at early time points, MTs are nucleated and polymerized from centrosomes and chromatin, whereas at later time points, MTs grow in their mass and bipolar spindles form. FAM29A is not required for MT nucleation and polymerization at early time points, but is essential for MT growth at later stages and for efficient formation of the bipolar spindle once sufficient amounts of MTs are polymerized. We propose that MT growth at later stages is derived from the MT-dependent MT polymerization in which FAM29A recruits the NEDD1–γ-tubulin complex to the mitotic spindle to promote additional MT polymerization. In this model, the FAM29A–NEDD1–γ-tubulin complex amplifies MTs in the spindle, thereby

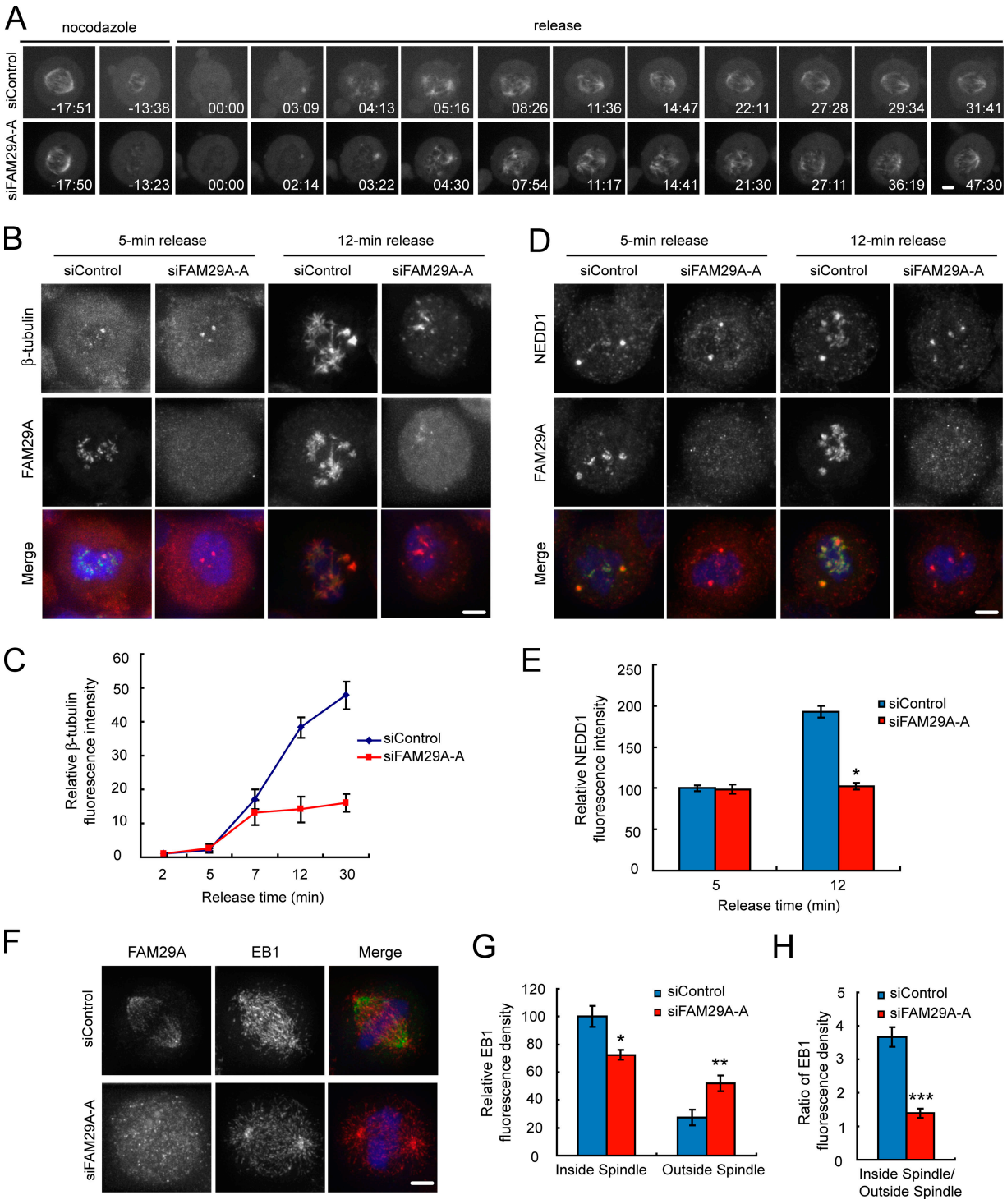

Figure 6. **FAM29A controls MT polymerization in the spindle.** (A) Still frames from confocal time-lapse microscopy of HeLa/GFP–α-tubulin cells transfected with siRNAs. Cells were treated with nocodazole for 15 min, washed with PBS, and released into fresh media (t = 0 min) (Video 9 for siControl and Video 10 for siFAM29A-A; Videos available at http://www.jcb.org/cgi/content/full/jcb.200807046/DC1). Time, min:sec. (B–E) HeLa cells transfected with siRNAs were treated with 1 µg/ml nocodazole for 15 min, washed, and released into fresh media for the indicated time. Shown are maximum projections from deconvolved z stacks of representative cells stained for FAM29A (green), β-tubulin (B)/NEDD1 (D) (red), and DNA (blue). Fluorescence intensities of β-tubulin (C) and NEDD1 (E) were quantified and plotted (n = 10 mitotic cells). *, $P < 0.003$ (two-tailed t test relative to siControl cells). (F–H) Maximum projections from deconvolved z stacks of representative HeLa cells transfected with siRNAs and stained for FAM29A (green), EB1 (red), and DNA (blue) (F). The EB1 fluorescence density inside and outside the spindle (G), as well as the ratio of inside vs. outside spindle (H) were quantified and plotted (n = 10 mitotic cells for each quantification). The EB1 fluorescence density is defined as the EB1 fluorescence intensity in a fixed circular area. *, $P < 0.005$; **, $P < 0.008$; ***, $P < 0.003$ (two-tailed t test relative to siControl metaphase cells). Error bars, SEM. Bars: 10 µm (A); 5 µm (B, D, and F).

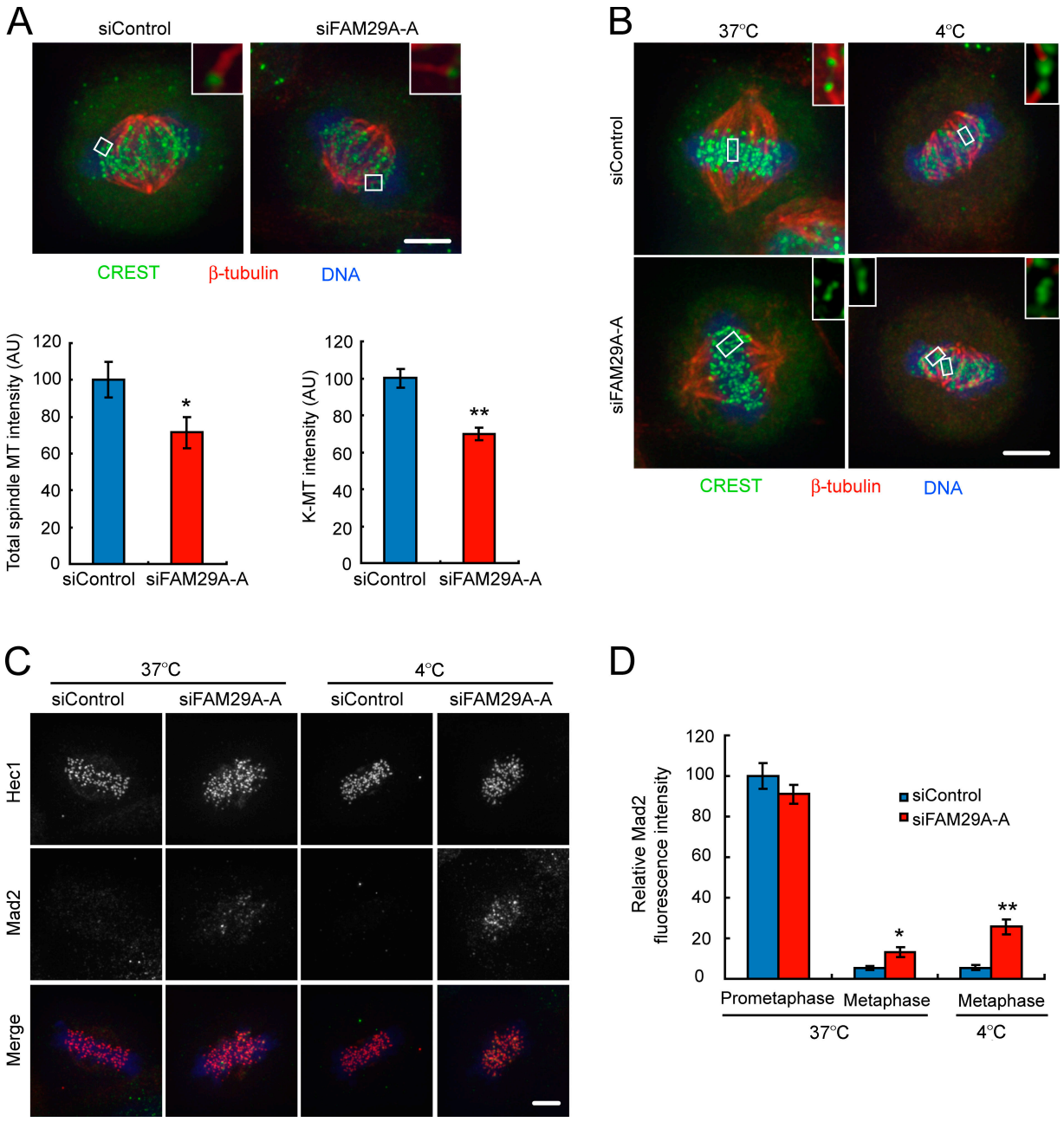

Figure 7. **FAM29A controls the maturation of kinetochore MT fibers.** (A) HeLa cells transfected with siRNAs were incubated at 4°C for 10 min, fixed, and stained for CREST (green), β-tubulin (red), and DNA (blue). Shown are maximum projections from deconvolved z stacks of representative cells. Insets show single focal planes of the boxed regions. Total intensity of spindle MTs as well as the intensity of k-MTs (the MT signal from a defined area immediately next to the CREST signal) were quantified and plotted (n = 10 metaphase cells for each quantification). *, $P < 0.05$; **, $P < 5.6 \times 10^{-5}$ (two-tailed t test relative to siControl metaphase cells). AU, arbitrary units. (B–D) HeLa cells transfected with siRNAs were incubated at 37°C or at 4°C for 10 min, fixed, and stained for CREST (B)/Mad2 (C and D) (green), β-tubulin (B)/Hec1 (C and D) (red), and DNA (blue). Shown in B and C are maximum projections from deconvolved z stacks of representative cells. Insets show single focal planes of the boxed regions. Fluorescence intensities of kinetochore Mad2 in prometaphase or metaphase cells under different conditions were quantified and plotted in D (n = 120 kinetochores). For metaphase cells in D, only kinetochores on chromosomes aligned at the metaphase plate were quantified. *, $P < 1.06 \times 10^{-4}$; **, $P < 1.14 \times 10^{-7}$ (two-tailed t test relative to siControl metaphase cells). Error bars, SEM. Bars, 5 µm.

efficiently increasing the MT mass for timely formation of the bipolar spindle. Depletion of FAM29A prevents this MT amplification and delays the spindle formation.

This model predicts that depletion of FAM29A does not interfere with initial recruitment of NEDD1 to centrosomes and chromatin, but prevents the association of NEDD1 with newly synthesized MTs. In the presence of nocodazole, NEDD1 remained at centrosomes independent of FAM29A (unpublished data). Furthermore, within 5 min of release from nocodazole treatment, NEDD1 was efficiently targeted to chromatin foci in both control and FAM29A-depleted cells (Fig. 6 D). In control mitotic cells, the intensity of NEDD1 signals increased over time, when increasing amounts of FAM29A were recruited to the growing MT mass. In contrast, in mitotic cells depleted of FAM29A, the

amounts of NEDD1 associated with spindle poles and chromatin did not increase over time (Fig. 6, D and E). These data supported our model in which FAM29A promotes MT amplification through the recruitment of the NEDD1–γ-tubulin complex to the mitotic spindle in a manner independent of centrosomes and chromatin.

Our study suggests a role of FAM29A-mediated MT amplification in spindle assembly during unperturbed mitosis. EB1 is a MT plus end–tracking protein that associates with the ends of growing MTs (Mahoney et al., 2006). We used EB1 as a cellular marker to monitor growing MT ends. In control metaphase cells, EB1 was predominately localized as punctates throughout the entire spindle and on spindle poles with minimal signals outside the mitotic spindle (Fig. 6 F). However, in FAM29A-depleted cells, the intensity of spindle EB1 punctates appeared much dimmer (by 30%) (Fig. 6, F–H), indicating a substantial reduction in the number of growing MTs. Furthermore, the EB1 signals outside the spindle increased in siFAM29A metaphase cells, approaching the intensity of EB1 inside the spindle. The EB1 around the spindle poles remained the same or increased in siFAM29A cells. These data are consistent with a model in which FAM29A plays a role in controlling the nucleation and growth of MTs within the spindle.

FAM29A controls the maturation of kinetochore MT bundles

Given that FAM29A is preferentially associated with k-MTs, we analyzed the role of FAM29A-mediated MT amplification in the formation of kinetochore MT fibers (k-fibers). HeLa cells were transfected with siFAM29A and incubated at 4°C to remove unstable nonkinetochore MTs, including the interpolar MTs that tend to associate with k-MTs at 37°C (Mastronarde et al., 1993). The intensity of individual k-fiber was then measured by the MT signal in a defined rectangle region immediately next to the attached kinetochore (Fig. 7 A). Compared with control cells, the k-MT signals were reduced by 30% in metaphase cells depleted of FAM29A, similar to the degree of reduction in total spindle MTs under cold treatment. Thus, depletion of FAM29A reduced the number of MTs attached to each kinetochore, suggesting that FAM29A-mediated MT amplification is required for the maturation of k-fibers.

Depletion of FAM29A not only reduced the average number of MTs attached to individual kinetochores, but also generated kinetochores without bound MTs on aligned chromosomes, even in cells without cold treatment (Fig. 7 B). Given that these attached chromosomes had already been aligned at the metaphase plate, we reasoned that these chromosomes were initially attached to k-MTs, but detached later due to the reduction in the number of k-MTs in FAM29A-depleted cells.

The checkpoint protein Mad2 monitors the state of MT attachment to kinetochores (Musacchio and Salmon, 2007). In prometaphase cells, kinetochores were not attached to MTs and had high levels of Mad2 signals independent of FAM29A depletion (Fig. 7 D). At metaphase, kinetochore Mad2 signals were reduced 10-fold in control cells due to MT attachment. However, Mad2 signals on kinetochores of aligned chromosomes were 2.5-fold higher in FAM29A-depleted cells than in control cells. Upon cold treatment, the Mad2 signal intensity remained the same in control metaphase cells, whereas the Mad2 intensity was further increased by twofold from 37°C to 4°C in metaphase cells depleted of FAM29A, indicating that cold treatment further destabilizes the weak attachment of k-MTs to kinetochores in the absence of FAM29A (Fig. 7, C and D).

To gain insights into the status of the MT attachment on individual kinetochores, we categorized kinetochores into four groups based on their Mad2 signal intensity (Fig. S5 C). Prometaphase kinetochores mostly fell into the group of the high Mad2 intensity and the distribution of kinetochores among these four groups was very similar between control and FAM29A-depleted prometaphase cells. However, kinetochores of chromosomes aligned at the metaphase plate in FAM29A knockdown cells had higher percentages that fell into higher Mad2 intensity groups than in control cells, and this difference is even greater upon incubation at 4°C. (Fig. S5 C). Thus, depletion of FAM29A increased the number of kinetochores that had weakly attached k-MTs. We conclude that FAM29A is required for the generation of mature k-fibers that stably attach to kinetochores.

Discussion

We report here that FAM29A is a spindle-associated protein required for the efficient capture of chromosomes, for the full tension across sister kinetochores, and for the timely onset of anaphase. Depletion of FAM29A generated disorganized mitotic spindles with a greatly reduced MT density. Biochemically, FAM29A interacts with the NEDD1–γ-tubulin complex. This interaction is dispensable for targeting NEDD1–γ-tubulin to centrosomes or chromatin, but is required for recruiting NEDD1–γ-tubulin to the spindle and for nucleating MTs from existing spindle MTs. Thus, FAM29A promotes MT polymerization in a process we termed MT-dependent "MT amplification", which represents a third MT nucleation mechanism that acts together with the centrosome- and chromatin-mediated MT polymerization in mitosis (Fig. 8 A) (Goshima et al., 2008). We showed that MT amplification contributes to the efficient spindle assembly and is critical for the maturation of k-fibers. The absence of FAM29A leads to thinner k-fibers and unstable kinetochore–MT attachments, which activate the spindle checkpoint and delay mitotic progression.

FAM29A in the assembly of the mitotic spindle and in the maturation of k-fibers

Centrosomes and chromatin are the two best-characterized centers of MT nucleation during mitosis (Gadde and Heald, 2004; Wiese and Zheng, 2006). Our data showed that nucleation of MTs from centrosomes and chromatin alone is not sufficient for the formation of stable bipolar spindles and that FAM29A-mediated MT polymerization is required for efficient spindle assembly and for stable bipolarity (Fig. 8, modules IIIa–c).

FAM29A is also crucial for the maturation of the k-fibers (Fig. 8, B and C). At prometaphase, individual MTs nucleated from centrosomes grow and shrink to search and capture individual kinetochore (Scholey et al., 2003). However, a mature kinetochore fiber consists of 25–30 MTs (McIntosh et al., 2002). FAM29A plays a key role in the formation of the mature kinetochore fiber from a single attached MT. In FAM29A-depleted

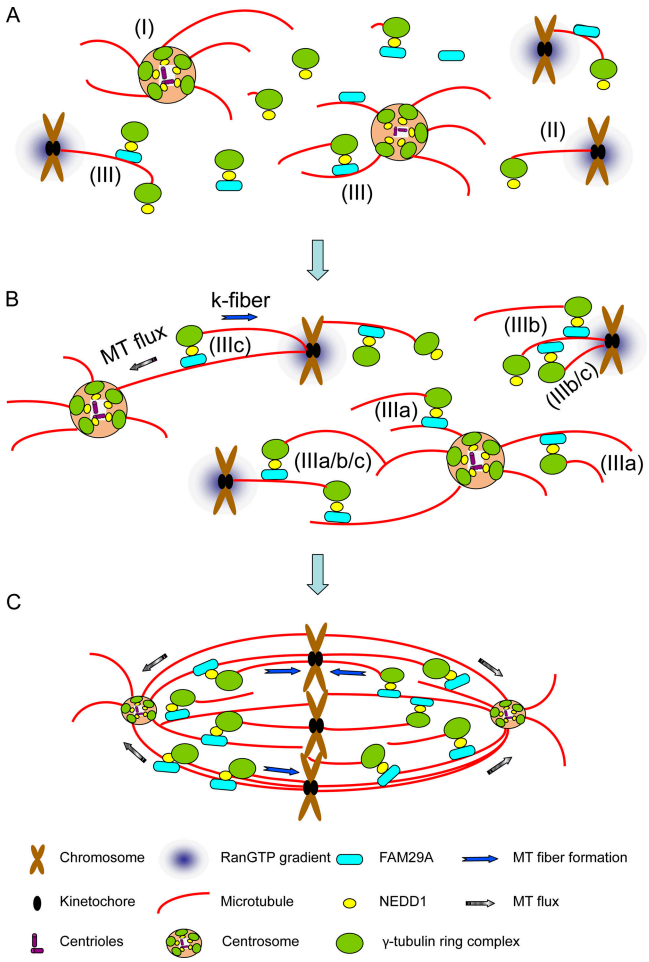

Figure 8. **A model for FAM29A-mediated MT amplification in spindle assembly and in k-fiber maturation.** (A) Three major pathways for MT nucleation in mitosis: centrosome-dependent (I), chromatin-dependent (II), and FAM29A/MT-dependent (III). (B and C) Role of FAM29A-mediated MT amplification in spindle assembly and in k-fiber maturation. FAM29A recruits the NEDD1–γ-tubulin complex to MTs derived from centrosomes and chromatin to promote their amplification (IIIa and IIIb, respectively). Similarly, FAM29A also targets the NEDD1–γ-tubulin complex to a kinetochore MT, which then nucleates additional MT to promote k-fiber maturation (IIIc). MT flux then transports newly synthesized MTs to spindle poles. Drawings for various cellular structures are representative, but not to scale.

cells, bipolar spindles form and the majority of chromosomes congress to the metaphase plate after a kinetic delay, indicating that k-fibers can form with a reduced level of FAM29A. However, the facts that FAM29A preferentially associates with k-fibers (Fig. 1) and that depletion of FAM29A reduces the k-MT intensity and weakens MT–kinetochore interactions (Fig. 7) provide evidence for a direct role of FAM29A-mediated MT amplification in the maturation of k-fibers. Our data support a model in which once a single MT captures a kinetochore and therefore is stabilized, the FAM29A pathway uses this attached MT as a template to quickly generate mature k-fibers, thereby displacing the checkpoint protein Mad2 and turning off the checkpoint signal from this kinetochore (Fig. 8 B, module IIIc). The poleward flux then actively transports the minus ends of MTs in the k-fiber toward the spindle pole to stably connect the pole to the kinetochore (Fig. 8 C).

Another source of k-fibers is MTs polymerized from chromatin, which are subsequently captured by spindle poles (O'Connell and Khodjakov, 2007). Chromatin-mediated formation of k-fibers can be directly analyzed in our MT repolymerization assay, as MTs repolymerized upon release from nocodazole treatment originate from BubR1-positive kinetochores (Fig. S5 D) (Tulu et al., 2006). Our data indicate that FAM29A-mediated MT amplification is also important for the maturation of k-fibers derived from chromatin (Figs. 6 and 8 B, module IIIb). We should also point out that although FAM29A preferentially associates with k-MTs, we cannot exclude the possibility that FAM29A also binds to and amplifies other MTs.

In addition to spindle assembly and k-fiber maturation, another M phase event that likely requires efficient MT amplification is the formation of central spindles at anaphase. Once chromosomes are segregated, the mitotic spindle disassembles and reorganizes into the central spindle of bundled MTs between two sets of segregating chromosomes (Mishima et al., 2002). It is likely that FAM29A-mediated MT amplification also plays a role here to promote efficient formation of the central spindle. This hypothesis is supported by the following observations. First, FAM29A and NEDD1 colocalized to the central spindle at anaphase (Fig. 1 B; Fig. S4 A). Second, depletion of FAM29A also reduced the NEDD1 signals on the central spindle (unpublished data). Third, depletion of FAM29A reduced the rate of chromosome segregation by 30% in anaphase (unpublished data).

Regulation of FAM29A

FAM29A is a cell cycle–regulated protein that functions in mitosis. The localization of FAM29A to spindle MTs only occurs in mitosis (Fig. 1). Similarly, although both FAM29A and NEDD1 proteins are present throughout the cell cycle, they only interact in mitosis (Fig. 5). Thus, the FAM29A–NEDD1 pathway is under active regulation, either through post-translational modifications or through an involvement of other uncharacterized factors. Interestingly, FAM29A was identified as a Plk1-interacting protein in our proteomic study, raising the possibility that Plk1 may control the FAM29A-mediated MT amplification.

We speculate that FAM29A-mediated MT amplification may function beyond the cell cycle in other physiological processes. For example, terminally differentiated neurons have axons and dendrites that are several feet away from centrosomes, and local organization of MTs using existing MTs as a template could be an efficient mechanism to reinforce the cytoskeleton structure through a positive feedback loop. Thus, MT amplification ensures a local regulation at places where MTs are needed. We propose that this important MT nucleation mechanism may act in many different physiological processes under different regulatory inputs that control the association of FAM29A with the MT cytoskeleton.

Materials and methods

Plasmids, antibodies, and cell lines

The full-length FAM29A was subcloned into the pCS2+ vector. GFP-FAM29A was subcloned into pCS2+ containing an N-terminal GFP tag. The eGFP-NEDD1 plasmid was provided by Jens Luders (Stanford University, Palo Alto, CA). Myc-NEDD1 was subcloned into pCS2+ containing an N-terminal Myc tag.

FAM29A fragments (aa 1–390, 390–718, 719–957) were subcloned into the pET28a vector (Invitrogen). The corresponding recombinant

proteins were expressed in *Escherichia coli*, purified, and used to immunize rabbits for the production of antisera. Antibodies were immunopurified using their respective immunogens. The rabbit anti-NEDD1 was provided by Jens Luders in the laboratory of Tim Stearns (Stanford University, Palo Alto, CA). The following antibodies were obtained from commercial sources: monoclonal anti-NEDD1 (Abnova Corporation); anti-GFP clone 3E6 (Invitrogen); anti–γ-tubulin clone GTU-88 (Sigma-Aldrich); CREST (Antibodies, Inc.); anti-Hec1 (GeneTex, Inc.); EB1 (BD Biosciences); and anti-p38MAPK, anti-Hsp70, and anti-cyclin B (Santa Cruz Biotechnology, Inc.). Rabbit antibodies against Mad2 and BubR1 were described previously (Fang, 2002; Jang et al., 2008). Anti–β-tubulin E7 monoclonal antibody was obtained from the Developmental Studies Hybridoma Bank (Iowa City, IA).

HeLa cells stably expressing GFP–Cenp-A was a gift from Jan M. Peters (Research Institute of Molecular Pathology, Vienna, Austria). HeLa cells stably expressing GFP–α-tubulin was provided by Linda Wordeman (University of Washington School of Medicine, Seattle, WA). GFP-FAM29A was subcloned into the pBabe vector and subsequently transfected into Phoenix-Ampho packaging cells. The viral supernatant was used to infect HeLa cells and stable clones were selected for 2 wk with 0.4 µg/ml puromycin. A clone that expressed the transgene below its endogenous protein level was used in this study.

Cell culture, siRNAs, and transfection

HeLa S3 and HeLa cells were cultured in DME containing 10% fetal bovine serum (Invitrogen) and antibiotics. Cells were synchronized at the G1/S boundary by a double-thymidine treatment or at prometaphase by a thymidine-nocodazole treatment (Fang et al., 1998a, b).

OnTargetPlus siRNAs were synthesized by Dharmacon, Inc. Sequences targeting FAM29A were (A) 5′-CAGTTAAGCAGGTACGAAATT-3′ and (B) 5′-CAACAAACGTCAAGCAATGTT-3′. Sequences targeting NEDD1 and Nuf2 were as reported previously (DeLuca et al., 2002; Luders et al., 2006). siRNAs were transfected into HeLa cells using DharmaFect 1 (Thermo Fisher Scientific). DNA transfection was performed using Effectene (QIAGEN).

Immunoprecipitation and immunofluoresence

Rabbit antibodies against GFP or FAM29A were coupled to Affi-Prep Protein A beads (Bio-Rad Laboratories) at a concentration of 0.3 mg/ml. HeLa or HeLa S3 cells were lyzed in NP-40 lysis buffer (50 mM Hepes, pH 7.4, 200 mM KCl, 0.3% NP-40, 10% glycerol, 1 mM EGTA, 1 mM $MgCl_2$, 0.5 mM DTT, 0.5 µM microcystin, and 10 µg/ml each of leupeptin, pepstatin, and chymostatin). Lysates were centrifuged, incubated at 4°C for 1 h with Protein A beads coupled with preimmune rabbit IgG, and then incubated at 4°C overnight with Protein A beads coupled with anti-GFP or anti-FAM29A antibodies. Antibody beads were recovered by centrifugation, washed four times with the lysis buffer in the presence of 500 mM KCl and once with the lysis buffer, analyzed by SDS-PAGE, and immunoblotted with appropriate antibodies.

HeLa cells on coverglasses were fixed with −20°C methanol for 5 min. Alternatively, cells were extracted with PHEMT buffer (60 mM PIPES, 25 mM Hepes, pH 6.9, 10 mM EGTA, 4 mM $MgCl_2$, and 0.5% Triton X-100) and then fixed with 4% paraformaldehyde for 15 min at room temperature. Subsequently, cells were permeabilized and blocked with PBS-BT (1× PBS, 3% BSA, and 0.1% Triton X-100) for 30 min at room temperature. Coverslips were then incubated in primary and secondary antibodies diluted in PBS-BT. Images were acquired with OpenLab 5.2 (Improvision) under a microscope (Axiovert 200M; Carl Zeiss, Inc.) using a 1.4 NA Plan-Apo 100x oil immersion lens. Deconvolved images were obtained using AutoDeblur v9.1 and AutoVisualizer v9.1 (AutoQuant Imaging).

Time-lapse microscopy and FLIP

For time-lapse microscopy, cells were cultured on coverglasses in Leibovitz's L-15 media (Invitrogen) supplemented with 10% FBS (Invitrogen) and 1× penicillin–streptomycin–glutamine (Invitrogen). Coverglasses were placed into a chamber heated to 37°C and observed under a microscope (Axiovert 200M; Carl Zeiss, Inc.) with a CCD camera (Orca-ER) and OpenLab 5.2. For confocal time-lapse microscopy, cells were observed using a 1.4 NA Plan-Apo 63× oil immersion objective (Carl Zeiss, Inc.) with a spinning disc confocal attachment (UltraView; PerkinElmer). In the MT depolymerization/repolymerization assays, metaphase cells were treated for 15 min with 1 µg/ml nocodazole in L-15 media at 37°C, quickly washed three times with 1× PBS prewarmed to 37°C, and reintroduced into fresh L-15 media. Images were acquired with OpenLab 5.2.

For the FLIP experiments performed in the laboratory of James Nelson (Stanford University, Palo Alto, CA), a coverglass with HeLa/GFP–α-tubulin cells was placed in a sealed chamber heated to 37°C. Cytoplasmic GFP–α-tubulin was photobleached with a fiber-optically pumped dye laser, and images were acquired at 0.5-s intervals for 300 s with SlideBook 4.0 (Intelligent Imaging Innovations) under an Axiovert 200M microscope with a 1.4 NA 100× oil immersion objective (Carl Zeiss, Inc.) and a CCD camera (CoolSnap HQ; Photometrics). 13 half-spindles for each transfection were analyzed by measuring the absolute GFP–α-tubulin fluorescence intensity in a defined circular area contained entirely within each half-spindle. Fluorescence intensities for each half-spindle were normalized to their maximum intensity at the beginning of the time lapse, and the 13 normalized datasets were averaged to generate a single trace for each condition. Half-lives for GFP–α-tubulin on the spindle were calculated by linear regression of the averaged traces.

In vitro MT assays

Assembly-competent α/β-tubulin was isolated as described previously (Hyman et al., 1991). Lysates of HeLa cells arrested at prometaphase by a thymidine-nocodazole treatment were incubated with 2 mM GTP, 10 µg/ml each of leupeptin, pepstatin, and chymostatin, 20 µM taxol, and 3.6 µM taxol-stabilized MTs in BRB80 buffer (80 mM Pipes, pH 6.8, 1 mM $MgCl_2$, and 1 mM EGTA) at room temperature for 30 min and pelleted at 100,000 *g* for 20 min at 30°C through a 150-µl 40% glycerol cushion containing 20 µM taxol and protease inhibitors in the BRB80 buffer. Pellets were washed three times with BRB80 buffer and analyzed by SDS-PAGE, followed by Western blotting.

In the MT visual assay, lysates of prometaphase HeLa cells were incubated with 2 mM GTP, 10 µg/ml each of leupeptin, pepstatin, and chymostatin, 20 µM taxol, and 3.6 µM taxol-stabilized MTs in BRB80 buffer at room temperature for 30 min. Samples were then fixed with 10 vol of BRB80 containing 1% glutaraldehyde at room temperature for 5 min, overlaid onto a 5-ml cushion (BRB80 plus 25% glycerol), and spun onto coverslips at 16,000 rpm for 70 min in a rotor (SW41Ti; Beckman Coulter) at 22°C. Coverslips were then fixed with −20°C methanol for 10 min and stained with indicated antibodies.

Sucrose gradient analysis of FAM29A

Lysates of HeLa cells arrested at prometaphase by a thymidine-nocodazole treatment were prepared in the absence of any detergent. A total of 20 µl lysates was loaded onto a 2.2-ml 10–40% sucrose gradient and centrifuged at 4°C in a rotor (TLS-55; Beckman Coulter) for 2.5 h at 55,000 *g*. Fractions were collected and analyzed by Western blotting. Aldolase (158 kD, 7S) and thyroglobulin (690 kD, 19S) (Bio-Rad Laboratories) were used as size markers and analyzed in parallel.

Online supplemental material

Fig. S1: knockdown of Nuf2 substantially reduces the spindle-associated FAM29A signals. Fig. S2: FAM29A controls mitotic progression. Fig. S3: FAM29A controls spindle structure. Fig. S4: FAM29A and NEDD1 colocalize and cofractionate. Fig. S5: FAM29A controls the structure and function of the mitotic spindle. Videos 1 and 2: FAM29A controls the duration of metaphase. Videos 3 and 4: FAM29A controls the inter-kinetochore distance and the movement of sister kinetochores relative to each other. Videos 5 and 6: FAM29A controls the rate of MT depolymerization upon nocodazole treatment. Videos 7 and 8: FAM29A controls the turnover rate of the mitotic spindle. Videos 9 and 10: FAM29A controls MT amplification. Online supplemental material is available at http://www.jcb.org/cgi/content/full/jcb.200807046/DC1.

We thank members of the Fang laboratory for discussions.

This work was supported by a Burroughs-Wellcome Career Award in Biomedical Research (G. Fang), by grants from the National Institutes of Health (GM062852 to G.Fang and HL079442 and RR11823-10 to J.R. Yates, III), and by Genentech, Inc. (G. Fang).

Submitted: 8 July 2008
Accepted: 31 October 2008

References

Barr, F.A., H.H. Sillje, and E.A. Nigg. 2004. Polo-like kinases and the orchestration of cell division. *Nat. Rev. Mol. Cell Biol.* 5:429–440.

Bastiaens, P., M. Caudron, P. Niethammer, and E. Karsenti. 2006. Gradients in the self-organization of the mitotic spindle. *Trends Cell Biol.* 16:125–134.

DeLuca, J.G., B. Moree, J.M. Hickey, J.V. Kilmartin, and E.D. Salmon. 2002. hNuf2 inhibition blocks stable kinetochore-microtubule attachment and induces mitotic cell death in HeLa cells. *J. Cell Biol.* 159:549–555.

Fang, G. 2002. Checkpoint protein BubR1 acts synergistically with Mad2 to inhibit anaphase-promoting complex. *Mol. Biol. Cell.* 13:755–766.

Fang, G., H. Yu, and M.W. Kirschner. 1998a. The checkpoint protein MAD2 and the mitotic regulator CDC20 form a ternary complex with the anaphase-promoting complex to control anaphase initiation. *Genes Dev.* 12:1871–1883.

Fang, G., H. Yu, and M.W. Kirschner. 1998b. Direct binding of CDC20 protein family members activates the anaphase-promoting complex in mitosis and G1. *Mol. Cell.* 2:163–171.

Gadde, S., and R. Heald. 2004. Mechanisms and molecules of the mitotic spindle. *Curr. Biol.* 14:R797–R805.

Goshima, G., M. Mayer, N. Zhang, N. Stuurman, and R.D. Vale. 2008. Augmin: a protein complex required for centrosome-independent microtubule generation within the spindle. *J. Cell Biol.* 181:421–429.

Gruss, O.J., and I. Vernos. 2004. The mechanism of spindle assembly: functions of Ran and its target TPX2. *J. Cell Biol.* 166:949–955.

Haren, L., M.H. Remy, I. Bazin, I. Callebaut, M. Wright, and A. Merdes. 2006. NEDD1-dependent recruitment of the gamma-tubulin ring complex to the centrosome is necessary for centriole duplication and spindle assembly. *J. Cell Biol.* 172:505–515.

Hyman, A., D. Drechsel, D. Kellogg, S. Salser, K. Sawin, P. Steffen, L. Wordeman, and T. Mitchison. 1991. Preparation of modified tubulins. *Methods Enzymol.* 196:478–485.

Jang, C.Y., J. Wong, J.A. Coppinger, A. Seki, J.R. Yates III, and G. Fang. 2008. DDA3 recruits microtubule depolymerase Kif2a to spindle poles and controls spindle dynamics and mitotic chromosome movement. *J. Cell Biol.* 181:255–267.

Janson, M.E., T.G. Setty, A. Paoletti, and P.T. Tran. 2005. Efficient formation of bipolar microtubule bundles requires microtubule-bound gamma-tubulin complexes. *J. Cell Biol.* 169:297–308.

Karsenti, E., and I. Vernos. 2001. The mitotic spindle: a self-made machine. *Science.* 294:543–547.

Kirschner, M., and T. Mitchison. 1986. Beyond self-assembly: from microtubules to morphogenesis. *Cell.* 45:329–342.

Kline-Smith, S.L., and C.E. Walczak. 2004. Mitotic spindle assembly and chromosome segregation: refocusing on microtubule dynamics. *Mol. Cell.* 15:317–327.

Luders, J., U.K. Patel, and T. Stearns. 2006. GCP-WD is a gamma-tubulin targeting factor required for centrosomal and chromatin-mediated microtubule nucleation. *Nat. Cell Biol.* 8:137–147.

Mahoney, N.M., G. Goshima, A.D. Douglass, and R.D. Vale. 2006. Making microtubules and mitotic spindles in cells without functional centrosomes. *Curr. Biol.* 16:564–569.

Maiato, H., J. DeLuca, E.D. Salmon, and W.C. Earnshaw. 2004. The dynamic kinetochore-microtubule interface. *J. Cell Sci.* 117:5461–5477.

Mastronarde, D.N., K.L. McDonald, R. Ding, and J.R. McIntosh. 1993. Interpolar spindle microtubules in PTK cells. *J. Cell Biol.* 123:1475–1489.

Mayer, T.U., T.M. Kapoor, S.J. Haggarty, R.W. King, S.L. Schreiber, and T.J. Mitchison. 1999. Small molecule inhibitor of mitotic spindle bipolarity identified in a phenotype-based screen. *Science.* 286:971–974.

McIntosh, J.R., E.L. Grishchuk, and R.R. West. 2002. Chromosome-microtubule interactions during mitosis. *Annu. Rev. Cell Dev. Biol.* 18:193–219.

Mishima, M., S. Kaitna, and M. Glotzer. 2002. Central spindle assembly and cytokinesis require a kinesin-like protein/RhoGAP complex with microtubule bundling activity. *Dev. Cell.* 2:41–54.

Murata, T., S. Sonobe, T.I. Baskin, S. Hyodo, S. Hasezawa, T. Nagata, T. Horio, and M. Hasebe. 2005. Microtubule-dependent microtubule nucleation based on recruitment of gamma-tubulin in higher plants. *Nat. Cell Biol.* 7:961–968.

Musacchio, A., and E.D. Salmon. 2007. The spindle-assembly checkpoint in space and time. *Nat. Rev. Mol. Cell Biol.* 8:379–393.

O'Connell, C.B., and A.L. Khodjakov. 2007. Cooperative mechanisms of mitotic spindle formation. *J. Cell Sci.* 120:1717–1722.

Petronczki, M., P. Lenart, and J.M. Peters. 2008. Polo on the rise-from mitotic entry to cytokinesis with Plk1. *Dev. Cell.* 14:646–659.

Pinsky, B.A., and S. Biggins. 2005. The spindle checkpoint: tension versus attachment. *Trends Cell Biol.* 15:486–493.

Scholey, J.M., I. Brust-Mascher, and A. Mogilner. 2003. Cell division. *Nature.* 422:746–752.

Seki, A., J.A. Coppinger, H. Du, C.Y. Jang, J.R. Yates III, and G. Fang. 2008a. Plk1- and beta-TrCP-dependent degradation of Bora controls mitotic progression. *J. Cell Biol.* 181:65–78.

Seki, A., J.A. Coppinger, C.Y. Jang, J.R. Yates, and G. Fang. 2008b. Bora and the kinase Aurora a cooperatively activate the kinase Plk1 and control mitotic entry. *Science.* 320:1655–1658.

Tulu, U.S., C. Fagerstrom, N.P. Ferenz, and P. Wadsworth. 2006. Molecular requirements for kinetochore-associated microtubule formation in mammalian cells. *Curr. Biol.* 16:536–541.

van Vugt, M.A., B.C. van de Weerdt, G. Vader, H. Janssen, J. Calafat, R. Klompmaker, R.M. Wolthuis, and R.H. Medema. 2004. Polo-like kinase-1 is required for bipolar spindle formation but is dispensable for anaphase promoting complex/Cdc20 activation and initiation of cytokinesis. *J. Biol. Chem.* 279:36841–36854.

Wiese, C., and Y. Zheng. 2006. Microtubule nucleation: gamma-tubulin and beyond. *J. Cell Sci.* 119:4143–4153.

Wilde, A., and Y. Zheng. 1999. Stimulation of microtubule aster formation and spindle assembly by the small GTPase Ran. *Science.* 284:1359–1362.

Wittmann, T., A. Hyman, and A. Desai. 2001. The spindle: a dynamic assembly of microtubules and motors. *Nat. Cell Biol.* 3:E28–E34.